AIAA JOURNAL
Vol. 31, No. 5, May 1993

Numerical Study of Shock-Wave/Boundary-Layer Interactions with Bleed

T. O. Hahn* and T. I-P. Shih†
Carnegie Mellon University, Pittsburgh, Pennsylvania 15213
and
W. J. Chyu‡
NASA Ames Research Center, Moffett Field, California 94035

A numerical study was conducted to investigate how bleed through a two-dimensional slot affects shock-wave induced, boundary-layer separation on a flat plate. This study is based on the ensemble-averaged, compressible, Navier-Stokes equations closed by the Baldwin-Lomax, algebraic turbulence model. The algorithm used to obtain solutions was the implicit, partially split, two-factored scheme of Steger. This study examined the effects of the following parameters in controlling shock-wave induced flow separation: location of slot in relation to where the incident shock wave impinged on the boundary layer, size of slot in relation to the boundary-layer thickness, number of slots, spacings between slots, and strength of the incident shock wave. This study also showed the nature of the very complex flowfield about the slot or slots and how the plenum affects the bleed process. The results of this study are relevant to problems where bleed is used to control shock-wave induced, boundary-layer separation (e.g., inside jet engine inlets and wind tunnels).

Introduction

SHOCK-WAVE/boundary-layer interactions and their control are known to play an important role in determining the successful operation of many aerodynamic and propulsion devices. Examples of such devices include inlets of jet engines, wind tunnels, and frames of supersonic aircraft. For these devices, shock-wave induced, boundary-layer separation can lead to severe consequences. For example, flow separation near throats of inlets can cause the unstart condition. For wind tunnels, flow separation creates flow distortion and reduces the effective Mach number in the test section. For supersonic aircraft, flow separation increases drag, reduces lift, and lowers the amount of air captured by the inlet for propulsion.

One effective way of controlling shock-wave induced, flow separation is to place bleed holes or slots in the vicinity where shock waves strike the boundary layer. These bleed apertures remove air near the wall surface where the momentum is low so that the remaining high-momentum air can withstand the high adverse pressure gradient created by the incident shock wave without separating.

The importance of bleed for controlling shock-wave/boundary-layer interactions has led a number of investigators to use both experimental and numerical methods to study this problem (see reviews by Delery[1] and Hamed and Shang[2]). According to Hamed and Shang,[2] although all experimental studies agree that bleed can control shock-wave induced, flow separation, disagreements exist between different experimental studies on how bleed-aperture size and location affect the amount of bleed needed to eliminate separation. These discrepancies indicate the complexities of the flow in the region about bleed holes or slots. In that region, many geometric and operating parameters can affect the flow physics with different parameters dominating under different conditions.

Hamed and Lehnig[3,4] performed a numerical study to address the discrepancy on how bleed-aperture location affects shock-wave/boundary-layer interactions on a flat plate. However, their study was based on only one two-dimensional slot geometry, one in which the depth of the slot is three times its width with the width equal to the displacement thickness just upstream of the interaction region. Also, they did not study the effects of the plenum on the bleed process. To date, numerical studies involving the plenum have not been reported. Also, the effects of the following parameters on the bleed process have not been investigated numerically: size of the bleed aperture, number of apertures, and spacings between apertures.

The objective of this investigation is to perform a numerical study of shock-wave/boundary-layer interactions on a flat plate with one or two two-dimensional slots that vent to a plenum. This study will account for the flow in the plenum as well as the flow above the plate and in the slot or slots. Also, it will examine the effects of the following parameters on the effectiveness of the bleed process in controlling shock-wave induced, boundary-layer separation: location of slot or slots in relation to where the shock wave impinged on the boundary layer, size of slots in relation to the boundary-layer thickness, number of slots, spacing between slots, and strength of the shock wave.

In the sections which follow, the shock-wave/boundary-layer interaction problem investigated is described first. Afterwards, the

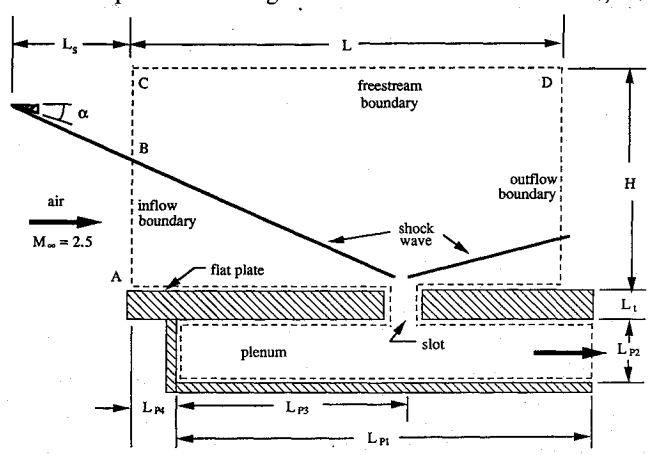

Fig. 1 Schematic diagram of problem studied. The dimensions are as follows: $L = 0.1778$ m (7 in.); $H = 0.0762$ m (3 in.); $L_t = 0.0015875$ m (1/16 in.); $L_{P1} = 0.142875$ m (5.625 in.); $L_{P2} = 0.0254$ m (1 in.); $L_{P3} = 0.0396875$ m (1.5625 in.); $L_{P4} = 0.06350$ m (2.5 in.); slot width and α are given in Table 1.

Received Feb. 15, 1992; revision received Sept. 9, 1992; accepted for publication Sept. 18, 1992.

*Graduate Student, Department of Mechanical Engineering.
†Associate Professor, Department of Mechanical Engineering. Member AIAA.
‡Research Scientist, Applied Aerodynamics Branch. Member AIAA.

formulation and numerical method of solution are given. Finally, results are presented which show details of the flowfield around bleed slots including the plenum and effects of the slot location and size on the bleed process.

Description of Problem

A schematic diagram of the shock-wave/boundary-layer interaction problem investigated in this study is shown in Fig. 1. Even though only one slot is shown, the number of slots that vent to the plenum can be one or two. The dash lines in Fig. 1 denote the boundary of the computational domain.

For the problem studied, the fluid was air with a constant specific-heats ratio γ of 1.4. The freestream Mach number M_∞, static temperature T_∞, and static pressure P_∞ were 2.5, 134 K, and 10.08 kPa, respectively. This supersonic flow had a turbulent, boundary layer next to the flat plate. At the inflow boundary, the thickness δ of that boundary layer was 0.03175 m (1/8 in.). A shock-wave generator characterized by L_s and α (see Fig. 1) caused an oblique, shock wave to strike the boundary layer. By varying α, the shock wave was made strong enough to cause boundary-layer separation. The parameter, L_s, controlled where on the boundary layer the shock wave impinged.

The interactions that took place as a result of the incident shock wave on the boundary layer was controlled via bleeding through either one or two slots. The back pressure P_b at the exit of the plenum was adjusted to give the minimum bleed rate that would eliminate as much as possible all separation induced by the oblique, shock wave. As will be described in the Results section, whether or not all separation can be eliminated by the bleed process depends on the location and size of the slot or slots.

In Fig. 1, most parameters such as L and H are self-explanatory and will not be described further. The exception is L_{P3}, and it is defined as the distance between the center of the slot or slots and the left wall of the plenum. Parameters not given numerical values in Fig. 1 such as slot width L_s and α are given in the Results section.

Formulation of the Problem

The shock-wave/boundary-layer interaction problem described in the previous section was modeled by the density-weighted, ensemble-averaged conservation equations of mass, momentum, and total energy written in generalized coordinates and cast in strong conservation-law form. The effects of turbulence were modeled by the Baldwin-Lomax algebraic turbulence model.[5] The momentum equations used were the thin-layer Navier-Stokes equations. Since the thin-layer Navier-Stokes equations account for diffusion only in directions normal to the streamwise direction, the computational domain shown in Fig. 1 was divided into three blocks—one for the region above the flat plate, one for the slot, and one for the plenum. For each block, a different coordinate system was used so that diffusion next to solid walls can be properly accounted for. When there are two slots, the computational domain was divided into four blocks with four different appropriately chosen coordinate systems.

To obtain solutions to the conservation equations, boundary and initial conditions are needed. The boundary conditions (BCs) employed in this study for the different boundaries shown in Fig. 1 were as follows. At the inflow boundary where the flow is supersonic everywhere except for a very small region next to the flat plate, two types of BCs were imposed. Along segment A-B, all flow variables were specified at the freestream conditions except for the streamwise velocity which had a velocity profile described by the one-seventh power law. With the one-seventh power law, the Reynolds number based on the displacement thickness at the inflow boundary was 59,000. Along segment B-C, postshock conditions based on inviscid, oblique, shock-wave theory were specified. These postshock conditions were also specified along the freestream boundary (segment C-D). At the outflow boundary where the reflected shock wave exits the computational domain, the flow is also mostly supersonic except for a thin region next to the wall. For that boundary, all flow variables were extrapolated by using three-point, backward differencing.

At all solid surfaces except the left wall of the plenum, the following viscous BCs were applied: no-slip condition, adiabatic wall, and zero normal-pressure gradient. At the left wall of the plenum, viscous BCs cannot be applied because the thin-layer Navier-Stokes equations do not account for diffusion in the streamwise direction. At that boundary, the following inviscid BCs were applied: the component of velocity normal to the wall was set to zero; for the tangential component of the velocity, its first-derivative in the direction normal to the wall was set to zero; the wall was adiabatic; and the normal momentum equation was used to determine pressure.

At the exit of the plenum where the flow is subsonic, velocity and total energy per unit volume were extrapolated in the same manner as the variables at the outflow boundary, and a back pressure was imposed. The numerical value of the back pressure was adjusted over time to give the minimum amount of bleed that would eliminate as much as possible all flow separation induced by the incident shock wave. Since a finite amount of time is required for the flow about the slot to respond to changes in the plenum back pressure, the actual pressure imposed at the plenum exit was

$$P_{\text{exit}} = \begin{cases} P_b & \text{if } |\phi| \le 0.05 \\ P_b + 0.4\phi, & \text{otherwise} \end{cases}$$

where P_b is the desired back pressure; $\phi = \dot{m}_{\text{plenum}} - \dot{m}_{\text{bleed}}$; $\dot{m}_{\text{plenum}}$ is the mass flow rate leaving the plenum at its exit; and $\dot{m}_{\text{bleed}}$ is the mass flow rate leaving the slot or slots. By using the above BC for pressure at the plenum exit, convergence to a steady-state solution was found to be accelerated considerably whenever the plenum back pressure P_b was changed.

Even though only steady-state solutions were of interest, initial conditions were needed because the unsteady form of the conser-

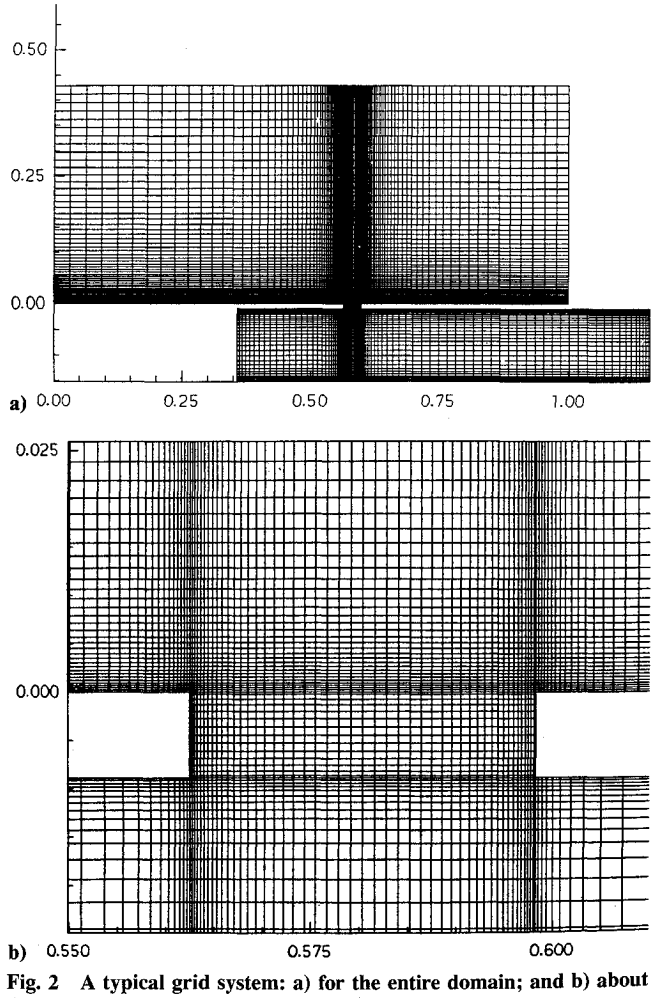

Fig. 2 A typical grid system: a) for the entire domain; and b) about the bleed hole.

Table 1 Summary of cases studied[a] and some key results

Case no.	Location of slots	No. of slots	Width of each slot,[b] 10^{-3} m	Spacing between slots, 10^{-3} m	Separation eliminated?	Bleed rate used, kg/s-m	P_b/P_∞
1	At shock	1	3.175	N.A.	Yes	0.0205	1.623
2	After shock	1	3.175	N.A.	No	0.0478	1.819
3	Before shock	1	3.175	N.A.	No	0.0281	0.487
4	At shock	1	6.350	N.A.	No	0.0249	1.707
5	At shock	1	1.5875	N.A.	Yes	0.0136	1.787
6	At shock	1	0.396875	N.A.	Yes	0.0134	0.420
7	At shock	1	0.28448	N.A.	No	0.00585	0.195
8	At shock	2	0.79375	0.79375	Yes	0.0172	1.749
9	At shock	2	0.79375	1.5875	Yes	0.0192	1.714
10	At shock	1	1.5875	N.A.	Yes	0.00108	1.269
11	At shock	1	1.5875	N.A.	N.A.	N.A.	N.A.

[a]For all cases, the freestream Mach number M_∞, pressure P_∞, and temperature T_∞ are 2.5, 10.08 kPa, and 134 K, respectively. For cases 1–9, the shock generator angle α is 8 deg; for case 10, $\alpha = 6$ deg; and for case 11, $\alpha = 4$ deg. N.A. = not applicable.

[b]The width of each slot is proportional to boundary-layer thickness δ at 10 cm upstream of slot. δ at that location is 3.175×10^{-3} m.

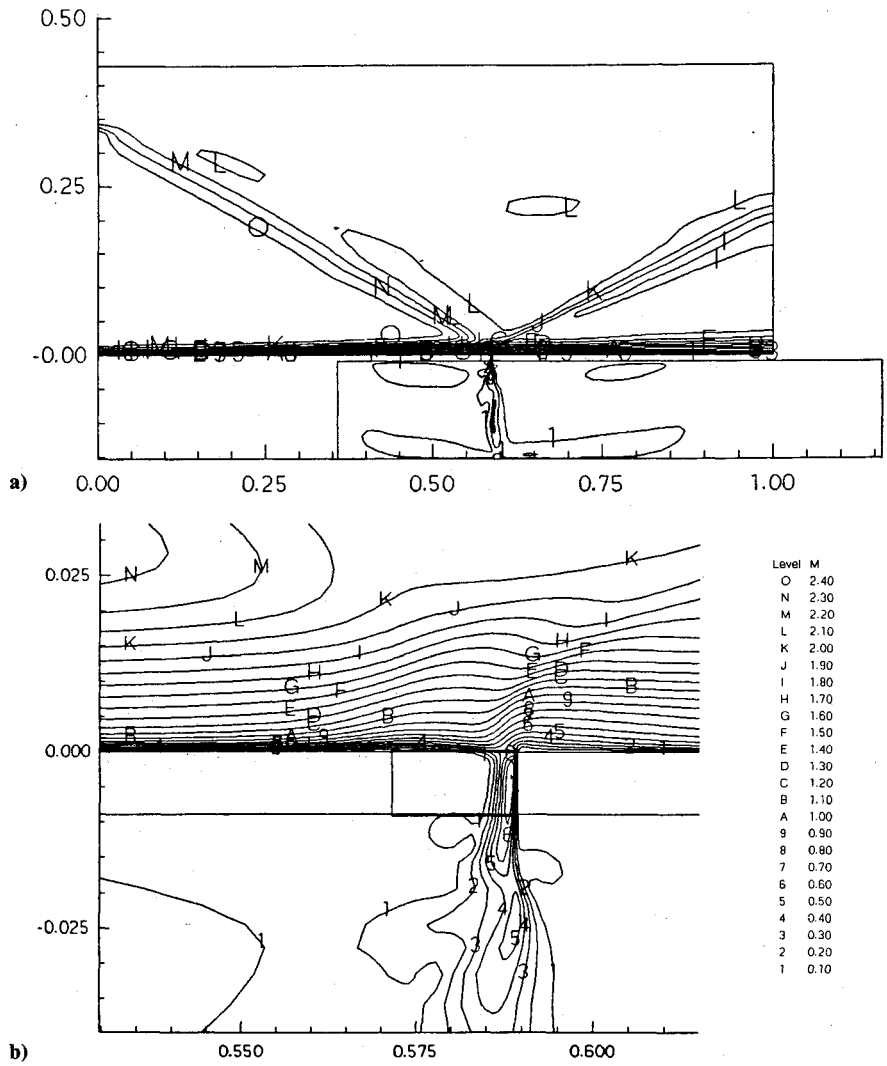

Fig. 3 Mach number contours for case 1 of Table 1 [contour levels defined in (b)]: a) for the entire domain; and b) about the bleed hole.

vation equations was used. The initial conditions employed in this study were as follows. In the region above the flat plate, the initial condition was the two-dimensional, steady-state solution for an incident and reflected oblique shock wave on a flat plate based on inviscid, shock-wave theory. However, the streamwise velocity profile next to the plate was modified to give the one-seventh power law. This necessitated the total energy per unit volume to be modified as well in order to account for the change in mechanical energy within the boundary layer. The initial conditions used in the slot or slots and the plenum were stagnant air at constant temperature and pressure.

Numerical Method of Solution

Solutions to the ensemble-averaged conservation equations of mass, momentum, and total energy closed by the Baldwin-Lomax algebraic turbulence model described in the previous section were obtained by using the F3D code developed by Steger et al. at NASA Ames Research Center.[6] The F3D code uses a partially split, two-factored, finite difference algorithm. In F3D, all convection terms in the streamwise direction were upwind differenced by using the flux-vector splitting scheme of Steger and Warming.[7] All convection and diffusion terms in directions normal to the streamwise direction were centrally differenced.

As mentioned in the previous section, the computational domain shown in Fig. 1 was divided into either three or four blocks depending upon the number of slots in order to account for diffusion correctly when using the thin-layer Navier-Stokes equations. In this division, all contiguous blocks overlapped each other by two grid lines. During computations, flow in each block is analyzed, one at a time in the following order: the block above the flat plate, the block in the slot, the block in the second slot if there are two slots, and the block in the plenum. Information from one block was transferred to another block via data computed on a previous block on one of the two common grid lines. This process of analyzing the flow in one block at a time until all blocks are analyzed is repeated for each timestep until a converged solution is obtained. Here, a solution is assumed to be converged if the second norm of the residual levels out for at least 1000 timesteps. At that time, the second norm was typically 10^{-7}. Here, it is noted that the residual oscillates about some averaged mean value as it levels out, and the amplitude of those oscillations were less than 10^{-7}.

The grid systems needed by the numerical method of solution were generated by using stretching functions. In this study, several different grid systems were employed because of the different slot geometries examined. All grid systems employed were arrived at via a grid-refinement study which involved doubling the number of grid points and comparing results. For each of the grid systems employed, the minimum grid spacing was always less than 4.2×10^{-5} m, and the maximum grid spacing never exceeded 5.7 $\times10^{-3}$ m. A typical grid system is shown in Fig. 2. The grid system shown in Fig. 2a has 157×75 grid points in the region above the plate, 29×49 grid points in the slot, and 135×41 grid points in the plenum. Figure 2b shows the details of the grid system about the slot.

Note that in Fig. 2, the spatial dimensions were nondimensionalized by L (=0.1778 m) as indicated by the coordinate system. The purpose of this coordinate system is to show the location in the computational domain where data is provided.

Results

Numerical solutions were generated to study the details of the shock-wave/boundary-layer interaction problem described in the previous sections. The effects of the following parameters were investigated: location of the slot or slots in relation to the shock wave (i.e., should the slot or slots be located before, at, or after where the shock wave impinged on the boundary layer), size of the slot in relation to boundary-layer thickness, number of slots, spacing between slots, and strength of the shock wave. Table 1 summarizes the cases studied along with some of the results obtained for them to be described later in this section. Each case was simulated in the following sequence in order to determine the minimum bleed rate needed to remove flow separation: First, the slot or slots were closed so that there was a significant separated region due to the shock wave impinging on the boundary layer. Afterwards, the

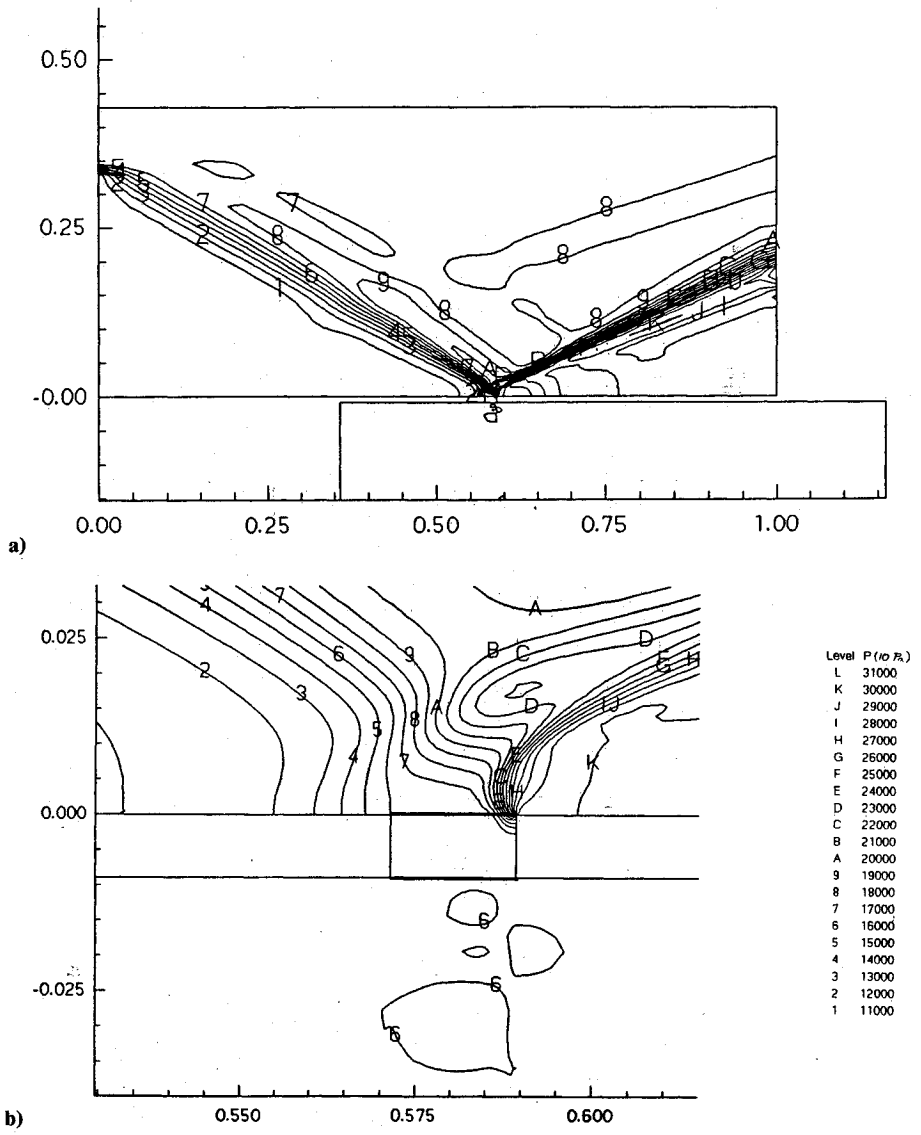

Fig. 4 Pressure contours for case 1 of Table 1 [contour levels defined in (b)]: a) for the entire domain; and b) about the bleed hole.

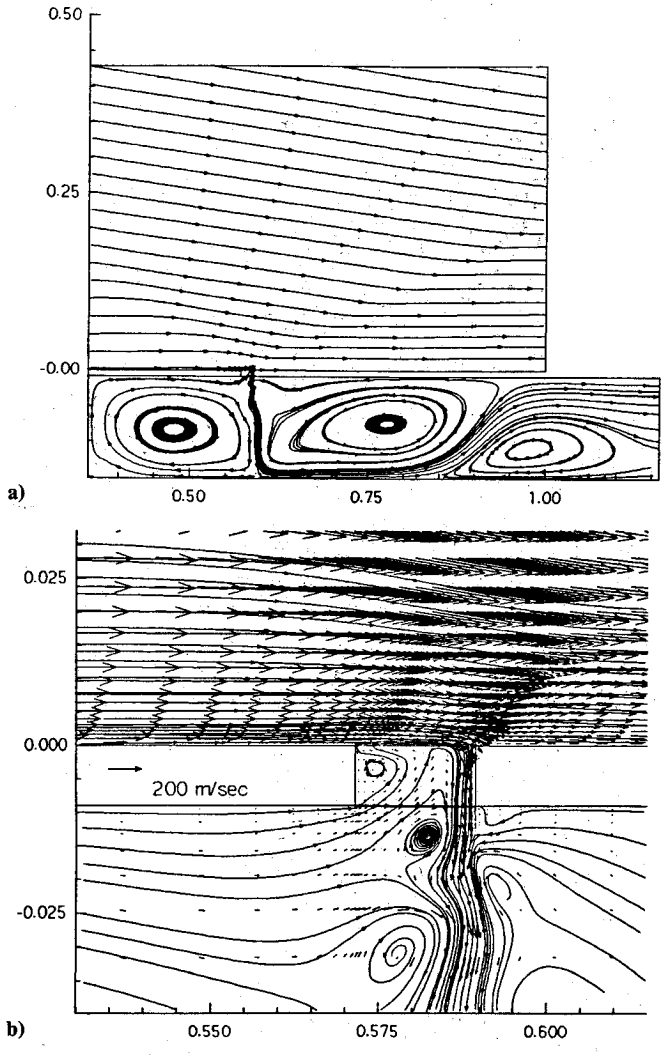

Fig. 5 Streamline contours with and without velocity vectors for case 1 of Table 1: a) for the entire domain; and b) about the bleed hole with velocity vectors.

slot or slots were opened, and the back pressure at the plenum exit was steadily lowered from the initial wall pressure to the value needed to remove as much as possible all flow separation.

Effects of Slot Location

Cases 1–3 in Table 1 were simulated to study the effects of slot location on the amount of bleed needed to remove shock-wave induced, flow separation. For all three cases, the slot size was 0.003175 m (1/8 in.), same as the thickness of the boundary layer just before the shock-wave/boundary-layer interaction region (henceforth referred to as the interaction region). Also, the angle of the shock generator (α) was set at 8 deg which was sufficient to induce significant flow separation in the absence of bleed. For case 1, the center of the slot was located at the inviscid-impingement point (i.e., the position where the shock wave would have impinged on the flat plate if there was no boundary layer). Since the boundary-layer thickness before the interaction region was 0.003175 m (1/8 in.) and the shock wave is known to curve inward once entering the boundary layer, the location where the shock wave actually impinged on the subsonic part of the boundary layer was slightly above and before the center of this slot. For cases 2 and 3, the centers of the slots were shifted by 0.003175 m (1/8 in.) after and before the inviscid-impingement point, respectively.

Results for cases 1–3 are shown in Figs. 3–7. For case 1, the shock-wave induced, flow separation can be eliminated completely by bleeding as can be seen in Figs. 3–5, and the minimum amount of bleed needed to remove the flow separation was found to be 0.0205 kg/s-m. The back pressure P_b corresponding to this bleed rate was 16.36 kPa which is higher than the pressure of the freestream before the interaction region (recall $P_\infty = 10.08$ kPa). Figures 3 and 4 show the location of the incident and reflected shock waves above the flat plate. From these figures, it can be seen that the interaction region is directly above the slot. Figures 3 and 5 show that bleeding only took place in a part of the slot, and that the flow there is subsonic. Figure 5 shows the very complex flowfield in the region about the slot and plenum. In that figure, three large vortical structures can be observed in the plenum. The two vortical structures on the left and right sides of the jet issuing from the slot were expected. The third vortical structure near the plenum exit was unexpected. That vortical structure was formed by a flow separation on the bottom wall of the plenum. The flow separated there because in that region the flow passage (bounded by the bottom wall of the plenum and the vortical structure on the right side of the jet) was effectively a diffuser which created an adverse pressure gradient.

For case 2, even at a bleed rate of 0.0478 kg/s-m with a P_b of 18.34 kPa, separation upstream of the slot cannot be eliminated as shown by Fig. 6. Higher bleed rates were not simulated since case 2 was clearly less effective than case 1 in eliminating separation by requiring more bleed. Note, even though the back pressure for this case was higher than that in case 1, the bleed rate was higher instead of lower. This is because the slot is located downstream of the shock-wave-impingement location where the pressure above the flat plate was considerably higher. For this case, bleeding created an oblique shock near the downstream end of the slot. This shock wave extends from the slot to slightly above the flat plate. The flow in the slot that passed through this shock is subsonic, and bleeding only took place in a part of the slot. Similar to case 1, vortical structures existed in the plenum but the number of vortices was four instead of three with the fourth vortex formed next to the top wall of the plenum near the exit.

For case 3, the slot was located upstream of the shock-wave-impingement location. For this case, a bleed rate of 0.0281 kg/s-m corresponding to a P_b of 4.94 kPa was unable to eliminate the flow separation which can be seen in Fig. 7. Since this bleed rate is higher than that in case 1, and separation remained, case 3, like case 2, was less effective than case 1 in eliminating separation. Similar to both cases 1 and 2, the bleeding only took place in a part of the slot, and vortical structures existed in the plenum. This case differed from case 2 but was similar to case 1 in that no shock wave was formed by the bleed process.

Comparing the results obtained for the three locations studied (cases 1–3), the best location for the slot in terms of minimizing bleed rate is the one directly below where the shock wave strikes the boundary layer (case 1).

Effects of Slot Width

Cases 1 and 4–7 were simulated to study the effects of slot width on the amount of bleed needed to remove shock-wave

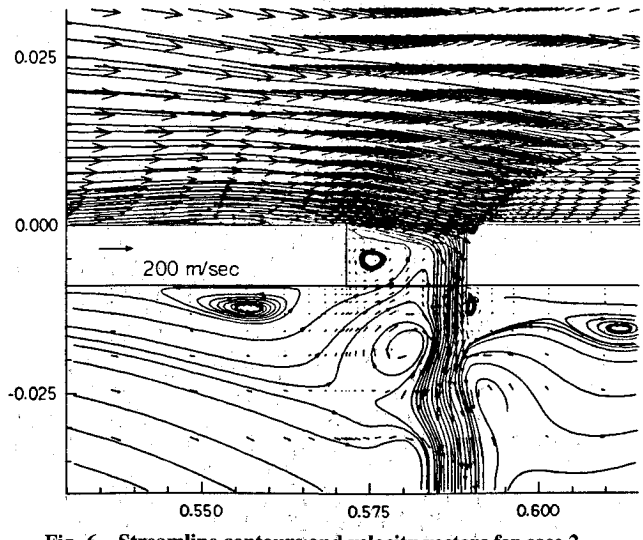

Fig. 6 Streamline contours and velocity vectors for case 2.

induced, flow separation (see Table 1 for the slot sizes investigated). For each of these cases, the slot was located at the inviscid-impingement point since that was found to be the optimum location in terms of minimizing bleed rate.

Recall that for case 1, the slot width was 0.003175 m (1/8 in.), same as the boundary-layer thickness just upstream of the interaction region. For cases 4 and 5, the slot size was twice and half that of case 1 (i.e., 0.006350 m and 0.0015875 m, respectively). For case 4, at a bleed rate of 0.0249 kg/s-m and a P_b of 17.21 kPa, the flow still separated because of blowing at the upstream edge of the slot as shown in Fig. 8. For this case, the slot extended across the interaction region from the low-pressure region upstream of the shock to the high-pressure region downstream of the shock. Thus, to eliminate flow separation, P_b had to be lowered below the freestream pressure P_∞, which would further increase bleed rate. This case was not studied further since it is clearly less effective than case 1 in eliminating flow separation.

For case 5, all flow separation can be eliminated at a bleed rate of 0.0136 kg/s-m and a P_b of 18.01 kPa as shown in Fig. 9. This bleed rate is 34% less than that in case 1—indicating that a smaller slot is more effective in eliminating flow separation than a larger one.

Now, the question is how small should the slot be before the slot becomes too small to eliminate flow separation. Cases 6 and 7 in Table 1 were simulated to study this. In case 6, the slot size was 0.000396875 m; in case 7, it was 0.00028448 m which was the same as the subsonic part of the boundary layer upstream of the

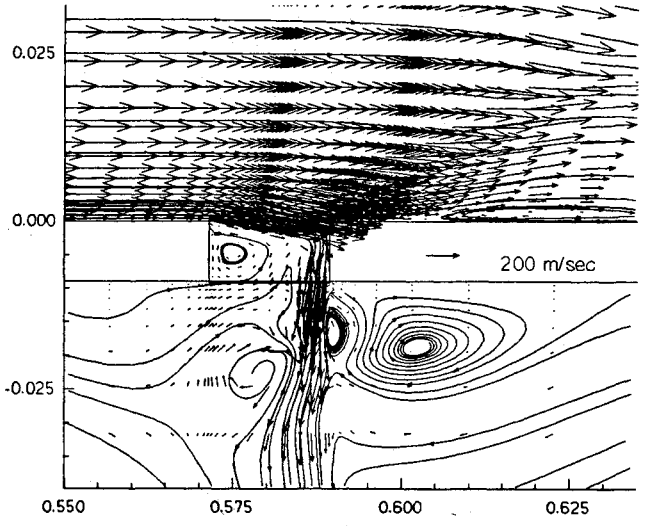

Fig. 7 Streamline contours and velocity vectors for case 3.

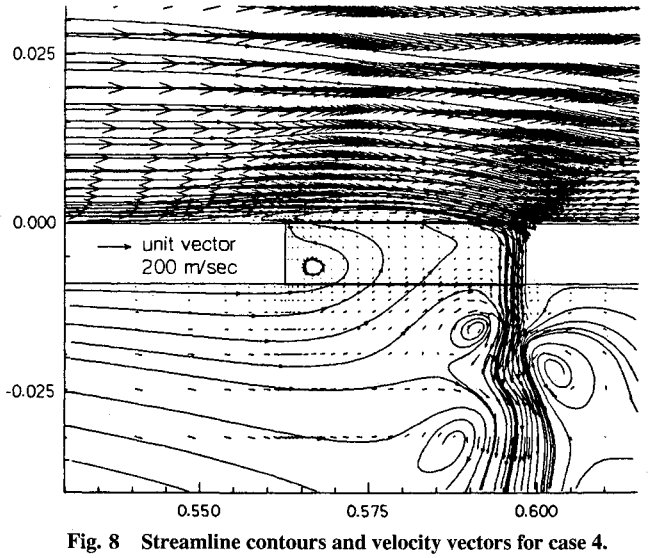

Fig. 8 Streamline contours and velocity vectors for case 4.

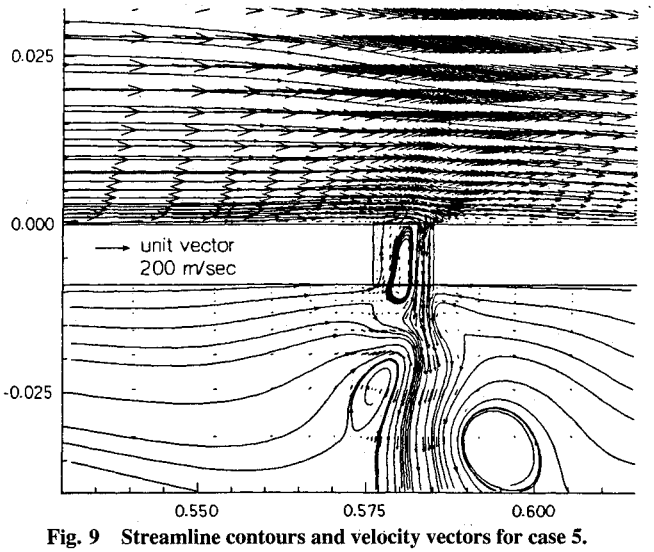

Fig. 9 Streamline contours and velocity vectors for case 5.

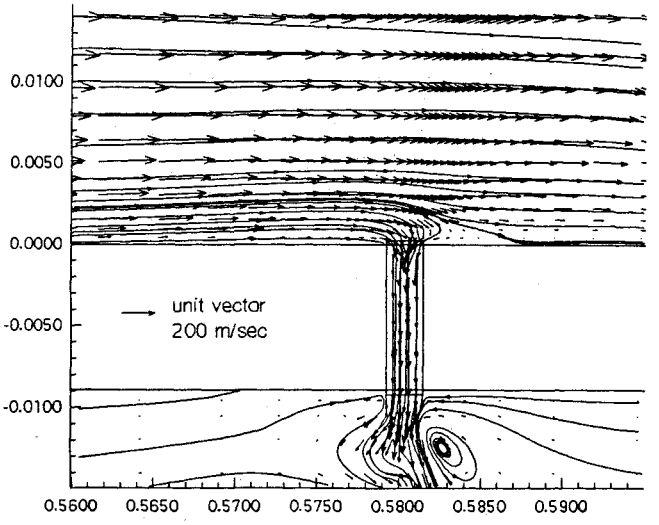

Fig. 10 Streamline contours and velocity vectors for case 6.

interaction region. For case 6, a bleed rate of 0.0134 kg/s-m with a P_b of 4.23 kPa was required to eliminate flow separation. This bleed rate is comparable to that obtained for case 5, and may represent the minimum bleed rate needed to remove flow separation for a slot positioned at this location. Figure 10 shows the flow field for case 6. From this figure, it can be seen that bleeding took place in the entire slot. For case 6, the maximum bleed rate that can be obtained was 0.0145 kg/s-m which is just slightly higher than that needed to eliminate separation.

For case 7, the maximum bleed rate was 0.00585 kg/s-m which is 45% less than the minimum required bleed rate for cases 1 and 6. At this bleed rate, P_b was 1.97 kPa; but flow separation cannot be eliminated as shown in Fig. 11.

The results obtained for cases 1 and 4–7 indicate that the slot size can be considerably smaller than the boundary-layer thickness but should be larger than the subsonic part of the boundary layer. The optimum size, of course, also depends on the boundary-layer profile (density and velocity) and the pressure ratio, P_b/P_∞, which were not investigated in this study.

Effects of Multiple Slots

Cases 5, 8, and 9 in Table 1 were used to study the effects of dividing a slot into two slots of equal size and varying the spacings between them. In cases 8 and 9, the single slot of case 5 with size 0.0015875 m was divided into two slots of size 0.00079375 m each. For case 8, the distance between the centers of the two slots was 0.0015875 m; for case 9, that distance was 0.0015875 m. Note that for both cases 8 and 9, the center of the two-slot region was

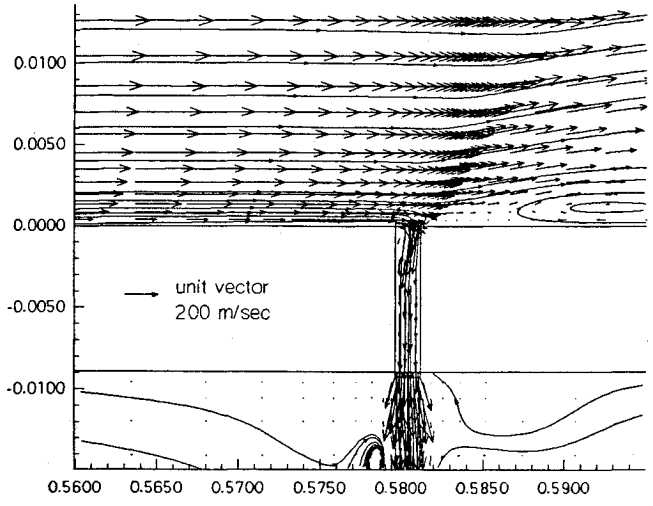

Fig. 11 Streamline contours and velocity vectors for case 7.

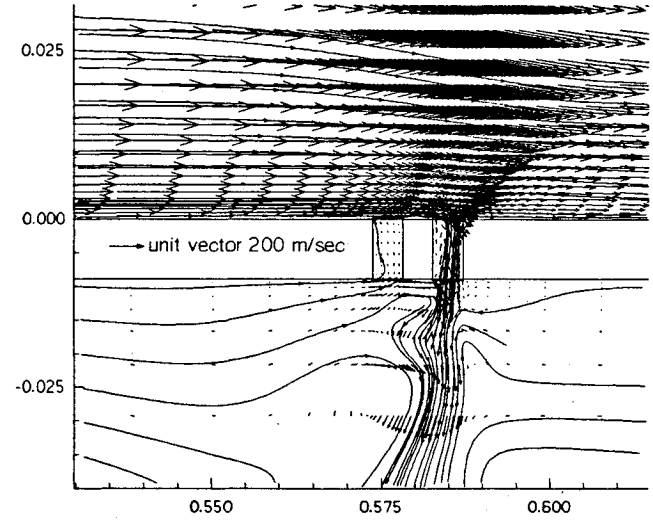

Fig. 12 Streamline contours and velocity vectors for case 8.

located at the inviscid-impingement point, same as the center of the slot for case 5.

The results for cases 8 and 9 are given in Figs. 12 and 13; these results can be compared with those of case 5 given in Fig. 9. For case 8, a bleed rate of 0.0172 kg/s-m achieved with a P_b of 17.63 kPa was required to eliminate all shock-wave induced, flow separation. To prevent the first slot (i.e., the one closer to the inflow boundary) from blowing air into the interaction region, a bleed rate of 0.0200 kg/s-m was needed. For case 9, a bleed rate of 0.0191 kg/s-m achieved with a P_b of 17.28 kPa was required to eliminate all shock-wave induced, flow separation, and a bleed rate of 0.0232 kg/s-m was needed to prevent blowing from the first slot.

Recall that for case 5, the bleed rate required to eliminate all shock-wave induced, flow separation was 0.0136 kg/s-m which is considerably lower than those required by cases 8 and 9. The reason for the increase in bleed rate for cases 8 and 9 is that the spacing between the slots allowed the slots to see different parts of the interaction region above the flat plate. This implies that lower plenum back pressures are needed in order to eliminate blowing from the first slot which sees the low-pressure part of the interaction region. But, a lower back pressure increases bleed rate through the second slot which sees the high-pressure part of the interaction region. Thus, if different slots are vented to the same plenum, then the effect of having several small slots is similar to having a single large slot spanning the same area. In this regard, case 9 can be compared with case 1 since the width of the slot for case 1 is only slightly larger than the distance spanned by the two slots in case 9. For cases 1 and 9, the bleed rates needed to remove shock-wave induced, flow separation were about the same. Also, the pressure and Mach contours were similar.

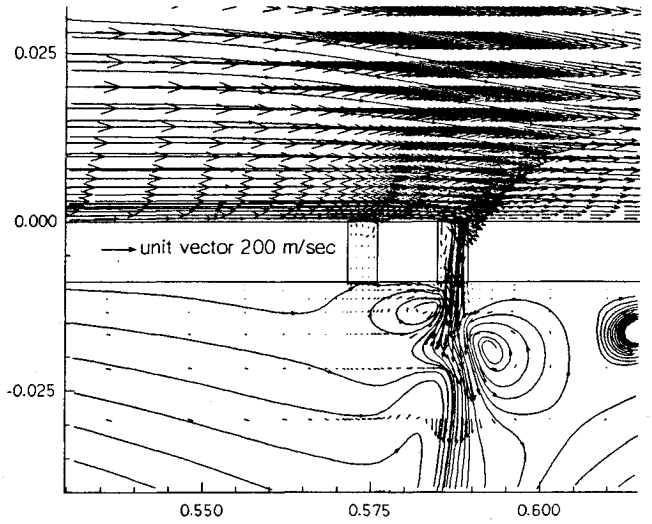

Fig. 13 Streamline contours and velocity vectors for case 9.

Effects of Slot Width/Depth Ratio

Cases 1 and 4–7 in Table 1 were used to examine the effects of the slot width/depth ratio on the flowfield. For cases 1, 4, and 5, the width/depth ratios are greater than or equal to unity. For these cases, Figs. 3–5, 8, and 9 show that bleeding only took place in a part of the slot with the other part occupied by a separation bubble which extended into the plenum (i.e., the separation bubble does not reattach in the slot). The size of this separation bubble was found to depend on the interactions that take place between the flow above the flat plate, in the slot, and in the plenum. This has important consequences on the bleed process in that even when there is a shock wave in the slot, the bleed rate can be increased by reducing the size of the separation bubble. Figures 3–5, 8, and 9 also show that when the width/depth is sufficiently high, blowing can take place at one end while bleeding takes place at the other end. Finally, streamlines that approach the slot curve less severely at higher width/depth ratios. For cases 6 and 7, the width/depth ratios are much less than unity. For these cases, Figs. 10 and 11 show that bleeding took place in the entire slot, and that the separation bubble reattached inside the slot. Under these circumstances, the bleed process is less affected by the plenum.

At this point, note that this study on the effects of width/depth ratio kept the boundary-layer thickness constant but not the ratio of slot width to boundary-layer thickness or the ratio of P_b to P_∞. Thus, further study is still needed.

Effects of Shock Strength

Cases 1, 10, and 11 in Table 1 were simulated to investigate the effects of shock strength on the bleed process. For these cases, all parameters were the same except for the angle of the shock wave which changed the pressure rise across the shock. For case 1, a fairly large separation region was induced by the shock wave in the absence of bleed. As noted earlier, the amount of bleed required to eliminate this separation was found to be 0.0205 kg/s-m. For case 10, a smaller separation region was induced since the shock strength was smaller than that of case 1. For this case, the amount of bleed needed to remove flow separation was 0.00108 kg/s-m. This smaller value is expected since the flow separation induced by the shock wave was smaller in size. For case 11, the shock strength was insufficient to induce any flow separation. Flowfield results for case 10 are not shown because the general features are very similar to those of case 1.

Summary

A numerical study was conducted to investigate how slot location and geometry affect the amount of bleed needed to control shock-wave induced, boundary-layer separation on a flat plate. This studied showed that placing a slot below where the shock

wave impinged on the boundary layer is optimum in terms of minimal bleed rate. Also, the slot width can be considerably smaller than the boundary-layer thickness but should be larger than the subsonic part of the boundary layer. If there are more slots than one, then the spacings between the slots should be kept as small as possible unless they vent to different plenums. Finally, the flow in the plenum can affect significantly the bleed rate if the width/depth ratio of the slot is sufficiently high.

At this point, several comments are in order. First, this study is far from exhaustive. For example, the optimum location and width also depend on the velocity and density profiles in the boundary layer as well as on the pressure ratio P_b/P_∞ which were not investigated. Also, minimal bleed rate is but one of several criteria that are important in applications involving bleed. Other criteria include the shape of the velocity profile after the bleed process. Finally, although efforts were made to assess the effects of grid spacings on the computed solutions, efforts were not made to assess the validity of the Baldwin-Lomax model used to describe turbulence. Thus, more work is still needed.

Currently, efforts are underway to study three-dimensional shock-wave/boundary-layer interactions on a flat plate with bleed through a circular hole and the effects of varying the pressure ratio P_b/P_∞.

References

[1]Delery, J. M., "Shock Wave / Turbulent Boundary Layer Interaction and Its Control," *Progress in Aerospace Sciences,* Vol. 22, 1985, pp. 209–280.

[2]Hamed, A., and Shang, J., "Survey and Assessment of the Validation Data Base for Shock Wave Boundary-Layer Interactions in Supersonic Inlets," AIAA Paper 89-2939, July 1989.

[3]Hamed, A., and Lehnig, T., "An Investigation of Oblique Shock/Boundary Layer/Bleed Interaction," AIAA Paper 90-1928, July 1990.

[4]Hamed, A., and Lehnig, T., "The Effect of Bleed Configuration on Shock/Boundary-Layer Interactions," AIAA Paper 91-2014, June 1991.

[5]Baldwin, B., and Lomax, H., "Thin-Layer Approximation and Algebraic Model for Separated Turbulent Flows," AIAA Paper 78-257, Jan. 1978.

[6]Steger, J. L., Ying, S. X., and Schiff, L. B., "A Partially Flux-Split Algorithm for Numerical Simulation of Compressible Inviscid and Viscous Flow," *Proceedings of the Workshop on Computational Fluid Dynamics,* Institute of Nonlinear Sciences, University of California, Davis, CA, 1986.

[7]Steger, J. L., and Warming, R. F., "Flux-Vector Splitting of the Inviscid Gasdynamic Equations with Application to Finite-Difference Methods," *Journal of Computational Physics,* Vol. 40, No. 2, 1981, pp. 263–293.